minerals

MDPI

Article

Assessment of Rare Earth Elements Fractionation in Sandstone and Magmatic Uranium Ores: Implications for Deposit Typing

Zhiger Kenzhetaev [1], Bolatbek Toksanbayev [1], Kuanysh Togizov [2,*], Kudaibergen Zhapabayev [1], Bagdara Mukatay [3], Madina Kurmangazhina [2] and Karina Svetlakova [2]

[1] Ascore, 30/10 Konaev Str., Tausamaly Microdistrict, Almaty 050067, Kazakhstan; kzhiger@yahoo.com (Z.K.); bolatbek_83@mail.ru (B.T.); zhapabaev.kudaibergen@mail.ru (K.Z.)
[2] Department of Geophysics and Seismology, Satbayev University, 22 Satbayev Str., Almaty 050013, Kazakhstan
[3] Department of Chemistry, Kazakh National Women's Teacher Training University, 99 Aiteke bi Str., Almaty 50000, Kazakhstan; mukatay.b@qyzpu.edu.kz
* Correspondence: k.togizov@satbayev.university

Abstract

This paper presents a comparative determination of rare earth elements (REEs) in sandstone-type uranium ore samples from Kazakhstan using a proposed rapid ICP-MS method following microwave digestion in a MARS 6 system with a mixed acid solution of HNO_3, HCl, and HF. To validate the rapid REE determination method, comparative measurements were performed using a certified uranium ore reference material provided by Ore Research & Exploration, representing sandstone-hosted uranium mineralization from a Tanzanian deposit (OREAS 120). Fractionation patterns of chondrite-normalized REEs in uranium ores from Kazakhstan were evaluated. Comparative data on REE distribution in sandstone- and magmatic-type uranium deposits from Australia and Tanzania are presented. Uranium ores of magmatic- and sandstone-hosted types exhibit distinct REE distribution patterns, reflecting differences in the nature of ore-forming processes. This study provides chondrite-normalized REE distribution profiles for major uranium deposit types from three countries, which are subsequently used to assess uranium ore paragenesis through simple linear regression analysis. This study is intended as an applied comparative synthesis of REE fractionation patterns in genetically contrasting uranium deposits, with particular relevance to deposit classification.

Keywords: REEs; rare earth elements; uranium ore; sandstone; ICP-MS; microwave digestion

1. Introduction

Existing analytical approaches for determining the elemental composition of uranium ores are generally focused on the quantification of specific elements using standardized and regulated analytical procedures. However, routine analytical practice often requires rapid and reliable multi-element determination. For this purpose, a range of analytical techniques is employed, among which inductively coupled plasma mass spectrometry (ICP-MS) and inductively coupled plasma atomic emission spectrometry (ICP-AES) are the most widely used due to their high analytical throughput and low detection limits. Since these techniques operate with liquid samples, particular attention must be paid to sample preparation procedures and instrument calibration.

In recent years, inductively coupled plasma mass spectrometry (ICP-MS) has become one of the leading methods for the investigation of geological materials, as it enables the

Check for updates

Received: 22 January 2026
Revised: 20 February 2026
Accepted: 16 March 2026
Published: 30 March 2026

Copyright: © 2026 by the authors. Licensee MDPI, Basel, Switzerland. This article is an open access article distributed under the terms and conditions of the Creative Commons Attribution (CC BY) license.

determination of ultra-trace concentrations for almost the entire range of trace and impurity elements in ores and minerals.

Inductively coupled plasma mass spectrometry (ICP-MS) is widely applied in geochemical studies in several analytical configurations. In addition to conventional solution nebulization ICP-MS, which requires complete sample dissolution and provides bulk compositional data, in situ microanalytical techniques such as laser ablation ICP-MS (LA-ICP-MS) are extensively used for spatially resolved analysis of minerals and rock components. In the present study, solution ICP-MS was selected to ensure complete digestion of uranium ores and to obtain representative bulk REE compositions suitable for comparative and forensic-style analysis.

Many uranium deposits in Kazakhstan are located within sedimentary basins, where rare earth elements (REEs) are incorporated into the mineral matrix. REEs are commonly associated with minerals such as monazite and bastnasite [1]. The most well-known uranium deposits of this type are situated within the Syrdarya and Chu–Sarysu uranium ore provinces [2].

Rare earth elements are widely recognized as key geochemical indicators of hydrothermal ore-forming processes. Uranium deposits span a broad range of geological ages, from the Archean to the Quaternary, and were formed under geochemical conditions varying from high-temperature magmatic to low-temperature exogenic environments [3].

In recent decades, data on REE distribution in ore minerals, together with stable isotope studies, have been extensively used to constrain the physicochemical parameters, composition, and sources of mineral-forming systems [4–8]. REE distribution patterns in calcium-bearing minerals (such as scheelite, fluorite, carbonates, and others) are particularly informative, as lanthanides have ionic radii similar to that of calcium and can readily substitute for Ca^{2+} in the crystal lattices of these minerals [9,10].

The objective of this study is to conduct a comparative analysis of REE fractionation in uranium ores from three deposits based on the investigation of REE elemental compositions in core samples. Analysis of REE distribution patterns in uranium ores allows refinement of deposit genesis, mineralization type, and potential sources of metals.

1.1. Mineralogical Characteristics of Sandstone-Hosted Uranium Deposits in Kazakhstan

As is well known, uranium production in Kazakhstan is predominantly carried out at sandstone-hosted deposits. Sandstone-type uranium deposits are characterized by the presence of associated rare and rare earth elements (REs and REEs) [11].

Uranium ores of southern Kazakhstan, particularly those of the Chu–Sarysu and Syrdarya provinces, are characterized by stratiform infiltration-type mineralization hosted in sandstones. Stratiform infiltration deposits are typical of the world's largest Pri-Tien Shan (East Turan) uranium ore province, which encompasses the Central Kyzylkum uplift (Uzbekistan), the Syrdarya Basin, and the Chu–Sarysu Basin (southern Kazakhstan) [12,13]. All these structures are located along the eastern periphery of the young Turan Plate and are commonly regarded as independent ore districts representing artesian basins composed of Upper Cretaceous, Paleogene, and Neogene sedimentary complexes.

The formation of deposits of this type is controlled by the circulation of oxygen-bearing infiltration waters, which precipitated dissolved and leached uranium together with associated elements at a reducing "geochemical barrier." A direct relationship is observed between ore grade and the reducing capacity of host rocks, which is determined by the presence of organic matter, pyrite, and other reducing agents. Uranium mineralization in these provinces is mainly represented by finely dispersed coffinite and uraninite (nasturan) [14]. The ores are predominantly non-carbonate in composition, with average uranium

contents ranging from 0.03 to 0.08%. The average mineralogical composition of uranium ores from southern Kazakhstan is presented in Table 1.

Table 1. Average mineralogical composition of uranium ore from southern Kazakhstan.

Mineral	Average Content, %
Quartz	data
Feldspars	65–75
Mica minerals (muscovite, biotite, chlorite, phlogopite)	7–15
Siderite	1–2
Calcite	1–2
Pyrite	1–3
Carbonized plant remains	1–5

Accessory minerals include tourmaline, ilmenite, leucoxene, staurolite, garnet, zircon, apatite, rutile, brannerite, kyanite, corundum, magnetite, hydrohematite, and limonite. Clay minerals are represented predominantly by hydromicas with admixtures of montmorillonite and kaolinite. The system of ore-controlling fronts of stratiform oxidation zones (SOZs) within the Upper Cretaceous horizons of the Syrdarya Province represents a systematic southern continuation of the corresponding system developed in the Cretaceous horizons of the Chu–Sarysu Province.

Uranium deposits of the Chu–Sarysu Province are known to be characterized by the presence of rare earth elements in the ore composition. REEs form highly stable oxides, halide compounds, and sulfides. Lanthanides are most commonly present as trivalent species, with cerium representing a notable exception due to its ability to readily oxidize to the tetravalent state. In addition to cerium, praseodymium and terbium are also capable of forming tetravalent compounds. Divalent compounds are known for samarium, europium, and ytterbium. In terms of physicochemical properties, lanthanides exhibit strong chemical similarity primarily due to their similar valence electron configuration and predominant trivalent oxidation state. The gradual filling of the inner 4f orbitals across the series results in the lanthanide contraction, which produces subtle but systematic differences in ionic radii and geochemical behavior.

The collective enrichment or depletion of the rare earth element group, variations in ratios between REE subgroups, and the presence of element-specific anomalies (most commonly europium and cerium) are widely used as sensitive indicators of mineral-forming processes [15,16]. Despite the overall coherence of rare earth elements, fractionation between light and heavy REEs may occur under specific geological conditions [15,17]. In geochemical practice, REEs are commonly subdivided into light REEs (LREE: La–Eu) and heavy REEs (HREE: Gd–Lu), with yttrium commonly grouped with HREEs due to its similar ionic radius and geochemical behavior [18,19]. Such differentiation may reflect variations in source composition, mineral hosts, and fluid–rock interaction processes.

Isomorphic substitution among rare earth elements, despite differences in their atomic numbers, is controlled by the phenomenon known as the “lanthanide contraction,” whereby increasing atomic number leads to filling of inner rather than outer electron shells, resulting in little to no increase in ionic volume.

Selective accumulation of REEs in minerals and rocks may be governed by differences in ionic radii. The ionic radii of lanthanides decrease systematically from lanthanum to lutetium, enabling preferential isomorphic substitution depending on the degree of size mismatch between substituting ions. Thus, scandium-, zirconium-, and manganese-bearing minerals may incorporate only REEs of the lutetium–dysprosium series; uranium minerals predominantly accumulate elements from the middle part of the series (yttrium, dysprosium, gadolinium); thorium minerals preferentially concentrate elements of the

cerium group; and only elements from the europium–lanthanum series may enter the structures of strontium- and barium-bearing minerals [20].

In the ores of hydrogeneous uranium deposits of Kazakhstan, the mineral association of nasturan (uraninite) and coffinite strongly predominates, although the ratio between uranium oxide and uranium silicate varies among individual deposits. Thus, coffinite overwhelmingly dominates at the South Moinkum, Irkol, and Zhalpak deposits, accounting for 90%–100% of the total uranium mineral assemblage. At the Tortkuduk deposit, the ratio of uranium silicate to oxide is approximately 65:35. A nearly equal proportion of oxide and silicate minerals is observed at the North Khorasan deposit. At the largest deposit, Mynkuduk, the ores are of the coffinite–nasturan type, with an average oxide-to-silicate ratio of 1.5:1. The proportion of nasturan increases from the Eastern sector to the Western sector of the deposit, reaching 2.5:1 in the latter.

Nasturan (uraninite) exhibits complex stoichiometry, incorporating Th, REEs, divalent elements (Pb, Ca, etc.), and uranium with higher oxidation states, which are commonly incorporated into its crystal structure during early crystallization and/or diagenesis [21–23]. The preferential incorporation of elements is largely controlled by similarities in ionic radii, with preference given to ions approaching the radius of U^{4+} (~1 A) in eightfold coordination, resulting in enrichment in Th^{4+} (1.05 A) and/or REEs (1.16–0.98 A) [24].

1.2. Characteristics of Magmatic–Hydrothermal Uranium Deposits in Australia

The formation of uranium deposits associated with magmatic systems is a multistage process involving magmatic differentiation, exsolution of a fluid phase, and subsequent hydrothermal–metasomatic alteration of host rocks. These deposits are interpreted as the result of uranium concentration in residual melts of highly evolved granitoid magmas followed by its mobilization by magmatic–hydrothermal fluids.

At the early stages of granitoid magma evolution, uranium occurs predominantly in the U^{4+} oxidation state and is incorporated into accessory minerals such as zircon, monazite, allanite, and titanite. During fractional crystallization, uranium, thorium, and rare earth elements progressively accumulate in the residual melt. As the magma becomes enriched in volatile components (H_2O, CO_2, F, Cl), magmatic–hydrothermal fluids are generated that are capable of transporting uranium in the form of stable complex species.

Migration of these fluids along fractures and fault zones leads to redistribution of uranium within surrounding rocks. Variations in temperature, pressure, and redox conditions promote a reduction of soluble U^{6+} to the less mobile U^{4+}, resulting in uranium precipitation, most commonly in the form of uraninite. Uranium mineralization is typically spatially associated with highly differentiated granites and accompanied by post-magmatic metasomatic processes such as albitization, greisenization, and K-feldspar metasomatism.

Thus, the formation of uranium deposits in magmatic systems is controlled by the interaction of magmatic evolution, fluid migration, and hydrothermal mineralization processes. Analysis of rare earth element distribution patterns and accessory mineral assemblages provides important constraints for reconstructing the formation conditions of such systems and refining genetic models of uranium mineralization.

2. Materials and Methods

The sample preparation procedure is described in detail in Ref. [25]. This article presents data from measurements of certified comparative materials, the certificates for which can be found on the Oreas website. Regarding core samples from Kazakhstan deposits, information on ore depth and deposit type is provided below. In this article, we used core samples from ore horizons of the following uranium deposits:

1. Inkai Deposit

Location: Turkestan Region, Shu-Sarysu Uranium Province
Deposit Type: Sedimentary, sandstone, roll-front (hydrogeochemical roll-front).
Ore horizon depth: Top of ore bodies: 350–400 m

2. Zarechnoye Deposit

Location: Kyzylorda Region, Syrdarya Province
Type: sandstone, roll-front
Ore depth: 300–450 m. The deposits are controlled by paleochannel structures. The ore is localized in Cretaceous aquifers. The hydrogeological parameters are relatively stable.

3. Zhalpak Deposit (part of the Shu-Sarysu Basin)

Location: Turkestan Region
Type: Sandstone uranium (roll-front)
Ore depth: 250–400 m. Medium-thick lenticular bodies. Hydrodynamically connected to the regional aquifer system.

4. Semizbay Deposit

Location: Northern Kazakhstan, Akmola Region
Deposit type: not sandstone, but vein (hydrothermal), associated with granite intrusions.
Ore depth: 100–150 m. Steeply dipping ore bodies, ranging in thickness from tens of centimeters to several meters. Higher uranium concentration compared to sandstone deposits.

5. Kharasan Deposit

Location: Kyzylorda Region, Syrdarya Province
Type: Sandstone, roll-front
Ore depth: 350–500 m. Complex hydrogeological conditions in individual blocks (variable mineralization of formation waters).

6. Mynkuduk Deposit

Location: Turkestan Region, Shu-Sarysu Province
Type: Sandstone
Ore depth: 300–450 m. Lens-shaped ore bodies extend along paleovalleys.

Measurements were performed using a quadrupole inductively coupled plasma mass spectrometer (ICP-MS), NexIon 350X (PerkinElmer), Shelton, CT, USA. The operating parameters of the ICP-MS instrument used during the experimental investigations are summarized in Table 2.

Corrections for polyatomic interferences were applied for the following rare earth elements (REEs):

- Nd 142 ($-0.125653 \times$Ce140);
- Sm 152 ($-0.12780 \times$Gd157);
- Gd 158 ($-0.040168 \times$Dy163);
- Dy 164 ($-0.047902 \times$Er166);
- 45Sc ($12C_{16}O_2$ $1H^+$, $28Si_{16}O_1H^+$, $29Si_{16}O^+$).

Calibration was performed using certified multi-element standard solutions supplied by PerkinElmer. Calibration standards and sample solutions for analysis were prepared immediately prior to measurements.

Table 2. ICP-MS instrumental operating parameters.

Instrumental Parameters		**Settings**	
Instrument	NexION 350X	Scan mode	Peak Hopping
Cones	Nickel	Channel per mass	1
Typical sensitivity, per mkg/L	9Be—5051cps 115In—48,062 cps U—52,468 cps Ce—55,529 cps CeO—1200cps Bkgd—0.4 cps	Dwell time per peak	50 ms
Plasma power	1400 W	Sweeps per read	20
Nebulizer gas flow	1.02 L/min	Total acquisition time	120 s
Auxiliary gas flow	1.2 L/min	Wash time	20 s
Plasma gas flow	17 L/min	Internal Standards (Rh)	50 mkg/L

Deionized water with a resistivity of 18.2 MΩ·cm^2, purified using an Arium 611 UF system (Sartorius, Göttingen, Germany), was used throughout the study. Nitric and hydrochloric acids of analytical grade, as well as hydrofluoric acid of analytical grade, were employed for sample digestion. Sample weighing was carried out using Sartorius MS Cubis analytical balances.

Microwave digestion of the samples was conducted using a MARS-6 microwave digestion system (CEM, Matthews, NC, USA).

To develop, analyze, and compare the performance characteristics of the proposed analytical method, as well as to evaluate REE fractionation patterns, certified reference materials and accompanying certificates provided by Ore Research & Exploration were used [26]:

- OREAS 120, a sandstone-hosted uranium ore reference material from the Mantra Resources Nyota Prospect, Tanzania. The OREAS 120 uranium ore standard is certified and registered within the State System for Ensuring the Uniformity of Measurements of the Republic of Kazakhstan;
- OREAS 100a, a uranium-bearing certified reference material from the Mount Gee uranium deposit of granite-hosted, hematite-type mineralization, Mount Painter Inlier, South Australia;
- OREAS 105, a medium-purity uranium reference material from the granite-type Crocker Well deposit, South Australia.

Europium (Eu) and cerium (Ce) anomalies were calculated using commonly accepted formulas:

$$Eu/Eu^* = EuN/\sqrt{(SmN \times GdN)},$$

$$Ce/Ce^* = 2CeN/(LaN + PrN),$$

where the subscript "N" denotes chondrite-normalized concentrations.

To develop, analyze, and compare the performance characteristics of the proposed analytical method, the uranium ore reference material OREAS 120 was used. The OREAS 120 uranium ore standard originates from the Nyota Prospect (Tanzania), operated by Mantra Resources, and represents an exogenic-type deposit. Mineralization occurs within medium- to very coarse-grained sandstones interbedded with greywackes and siltstones. The mineralogical and chemical composition of the matrix is comparable to the average characteristics of sandstone-hosted uranium ores from Kazakhstan.

The OREAS 120 reference material represents a stratiform sandstone-hosted deposit of the Karoo sequence. Mineralization is secondary in nature and is typically concentrated within medium- to very coarse-grained sandstone units containing interlayers of greywacke, siltstone, or argillite. On average, the ore consists of approximately 82% quartz, feldspar, and siliceous components, with aluminum oxide contents not exceeding 10 wt.%. Uranium mineralization is represented by two principal phases: nasturan (uraninite) and coffinite. The major macro-impurities are listed in Table 3.

Table 3. Major macro-impurities of the OREAS 120 uranium ore reference material.

Constituent	Certified/Value	SD
Al_2O_3, Aluminum(III) oxide (wt.%)	9.14	0.145
BaO, Barium oxide (ppm)	1088	44
Fe_2O_3, Iron(III) oxide (wt.%)	2.27	0.045
K_2O, Potassium oxide (wt.%)	3.31	0.049
MgO, Magnesium oxide (wt.%)	0.410	0.022
MnO, Manganese oxide (wt.%)	0.103	0.002
P_2O_5, Phosphorus(V) oxide (wt.%)	0.029	0.004
SiO_2, Silicon dioxide (wt.%)	81.86	0.603
TiO_2, Titanium dioxide (wt.%)	0.427	0.015
U, Uranium (ppm)	40.5	7.0

Sample Preparation for Analysis

Ore samples were digested in two stages. The total digestion time was approximately 3 h.

Stage 1 (primary digestion). Sample weight of 0.1 g was moistened with 0.25 mL of deionized water. Sample digestion was carried out using a MARS-6 microwave digestion system under the following conditions: pressure up to 35 bar and power of 800 W. A mixture of high-purity concentrated acids was added to each digestion vessel containing the sample: 1 mL HF + 1 mL HNO_3 + 4 mL HCl.

Microwave digestion was performed in two steps. Initially, we raise the temperature to 90–110 °C for 5 min, maintain this temperature for 15 min, then within 5 min we increase it to 200 °C and maintain it for 20 min. Upon completion of digestion, the vessels were allowed to cool inside the microwave system to a temperature range of 80–40 °C.

Stage 2 (secondary digestion). An acid mixture for the second digestion stage was prepared by mixing 1 mL HCl (azeotropic mixture, 20%), 1 mL HNO_3, and 5 (10) mL of 4% H_3BO_3. The digestion temperature was raised to 180 °C and maintained for 10 min, followed by cooling to room temperature. After complete cooling, an internal standard was added and the solutions were diluted to volume with deionized water. All resulting solutions were clear, indicating complete digestion of the samples.

The use of a mixture of hydrofluoric, hydrochloric, and nitric acids during the first digestion stage enables nearly complete transfer of the sample into solution, converting metal fluorides into chlorides. Cooling the digestion vessels to temperatures equal to or above 85 °C results in silicon loss, whereas cooling to temperatures equal to or below 35 °C leads to precipitation of insoluble fluorides of certain metals. Therefore, samples were cooled in sealed vessels to a temperature range of 80–40 °C.

During the second digestion stage, the use of a mixture of concentrated hydrochloric and nitric acids with diluted boric acid ensures complete dissolution of the samples, further decomposition of silica-rich matrices, and complexation of unreacted HF. The presence of boric acid creates conditions that prevent the formation of precipitating metal hydroxides upon subsequent dilution with water. Thus, boric acid acts as a buffering agent, suppressing hydrolysis of certain salts.

Microwave digestion using the MARS system allows the entire procedure to be conducted from start to finish within a single vessel, thereby reducing labor intensity, eliminating technological and volatile component losses, minimizing errors associated with sample preparation, and increasing the reliability of the analytical results.

3. Results and Discussion

Five subsamples of the OREAS 120 uranium ore reference material were selected. Concentrations of major elements (ME) and rare earth elements (REEs) were measured using the procedure described in the patent [25]. The obtained results fall within the confidence intervals of the certified values, confirming the effectiveness of the digestion procedure and the accuracy of the subsequent ICP-MS analysis.

The relative standard deviation for most elements does not exceed 10%, which is acceptable and sufficient for rapid measurements. It should be noted that concentrations of some major and rare earth elements in solution are underestimated relative to certified values due to matrix effects. This issue can be addressed using established analytical approaches, such as optimization of the internal standard, the method of standard additions, and related techniques [25].

Tables 4 and 5 present the mean concentrations of major elements and REEs measured for the OREAS 120 uranium ore reference material.

Table 4. Mean concentrations of elements measured in the OREAS 120 reference material.

Element	Ref, ppb	Mean, ppb	SD	RSD	M/Ref
Sc	2.730	3.077	0.2	8.5	1.127
Ti	2380	2726	244.5	9.6	1.145
Mn	780.0	761.1	13.3	1.7	0.976
Ni	8.220	7.348	0.6	7.9	0.894
Rb	88.00	96.15	5.7	6.3	1.093
Sr	124.0	138.2	10.0	7.7	1.115
Y	10.10	9.904	0.1	1.4	0.981
Nb	7.700	6.897	0.5	7.8	0.896
Mo	6.970	6.949	0.01	0.2	0.997
Ba	983.0	1023	28.3	2.8	1.041
U	39.60	34.62	3.5	9.4	0.874

Table 5. Mean concentrations of rare earth elements (REEs) measured in the OREAS 120 reference material.

Element	Ref, ppb	Mean, ppb	SD	RSD	M/Ref
La	20.3	18.25	1.5	7.5	0.90
Ce	44.5	39.85	3.3	7.8	0.90
Pr	5.20	4.477	0.5	10.6	0.86
Nd	19.4	16.62	1.9	10.9	0.86
Sm	3.82	3.480	0.2	6.6	0.91
Eu	1.11	1.107	0.002	0.2	1.00
Gd	3.14	3.202	0.04	1.4	1.02
Tb	0.43	0.404	0.02	4.5	0.94
Dy	2.29	2.056	0.2	7.6	0.90
Ho	0.42	0.373	0.03	8.5	0.89
Er	1.21	1.076	0.09	8.3	0.89
Tm	0.16	0.137	0.02	10	0.86
Yb	1.03	0.988	0.03	2.9	0.96
Lu	0.15	0.133	0.01	8.7	0.88

Based on the results obtained during the validation of the REE measurement method using the OREAS 120 uranium ore reference material, core samples from six uranium

deposits in Kazakhstan were analyzed using the same analytical approach. Five subsamples were collected from each core sample. REE fractionation in the core materials was subsequently evaluated. Chondrite normalization was applied to assess variations in lanthanide composition associated with hypogene processes, as the lanthanide composition of chondrites is considered to most closely represent that of the primary protoplanetary material [26].

In addition, to provide a comparative framework for REE fractionation, certificate data from two additional ore reference materials supplied by Ore Research & Exploration OREAS 100a and OREAS 105 were analyzed.

The uranium-bearing certified reference material OREAS 100a was prepared from material sourced from the Proterozoic Mount Gee uranium deposit, located within the Mount Painter Inlier, South Australia. Mineralization at Mount Gee occurs within the Paralana mineral system, which hosts a series of granitic and hematite breccia bodies. The Mount Gee deposit is interpreted as hydrothermal in origin and is commonly described as a variant of iron oxide–copper–gold (IOCG)-type mineralization.

The medium-purity uranium reference material OREAS 105 was prepared from samples collected from the Crocker Well project, situated in the Olary district of the Curnamona Province, South Australia. Uranium mineralization occurs within basement intrusive rocks, predominantly as thorium-bearing brannerite present as a disseminated accessory mineral or within fractures, breccias, and quartz veins hosted by sodium-rich plagioclase-bearing Mesoproterozoic granitoids and gneisses. Material from the Crocker Well deposit was blended with barren rhyodacite to achieve the target uranium concentration in OREAS 105.

Figure 1 presents chondrite C1-normalized REE distribution patterns for the analyzed core samples. Chondrite normalization is superior to other reference materials such as PAAS/NASC/UCC for assessing the degree of processing of uranium ore sedimentary material. CI chondrites reflect the original nebular REE distribution, the absence of crustal differentiation, and minimal fractionation. Essentially, this is the zero-level of geochemical evolution. Any deviations in the ore reflect actual fractionation processes, not the properties of the selected sedimentary reference material. PAAS/NASC/UCC sedimentary composites are already fractionated. They represent a mixture of weathered continental material that has already undergone magmatic differentiation and sedimentary sorting. Their spectra are enriched in LREE and exhibit a persistent negative Eu anomaly [27]. The total rare earth element contents in the core materials range from 50 to 100 g/t.

In most of the analyzed core samples, the chondrite-normalized $(La/Yb)_n$ ratio ranges from 3 to 6, accompanied by moderate fractionation of the middle to heavy REEs ($(Gd/Yb)_n$ = 1–1.9). This pattern indicates a predominance of felsic detrital material supplied to the sedimentary basin. A weakly developed negative europium anomaly ($Eu/Eu^* \approx 0.7$) is observed, which is typical of sedimentary systems enriched in felsic detritus and is also indicative of erosion of felsic source rocks. Thus, the combination of these geochemical parameters suggests a felsic composition of the provenance areas [28–31].

The REE distribution patterns shown in Figure 1 are characterized by enrichment in light lanthanides, the absence of pronounced differentiation between middle and heavy REEs, and a weak negative Eu anomaly. The subdued europium anomaly in sandstone-hosted uranium ores may be attributed to the sedimentary origin of the ores and the secondary nature of the ore-forming fluids. Under low-temperature groundwater transport conditions, rare earth elements, including europium, do not undergo significant fractionation.

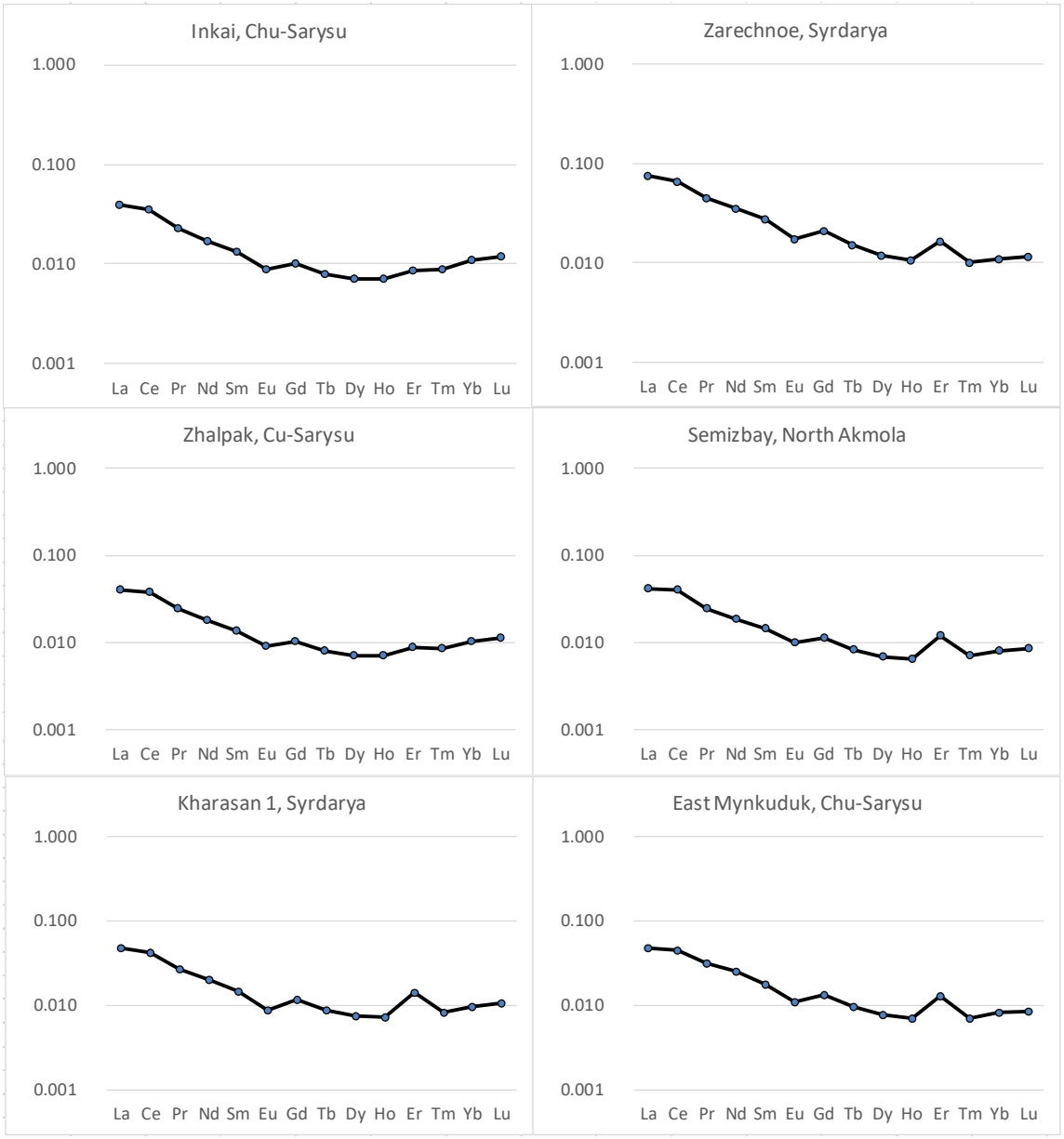


Figure 1. Chondrite-normalized REE distribution patterns in sandstone-hosted uranium ore cores from the Chu–Sarysu and Syrdarya basins (Kazakhstan), illustrating felsic provenance and weak REE fractionation typical of sedimentary uranium systems.

Minor deviations observed for individual middle and heavy REEs, such as slight Er or Gd anomalies, may reflect the presence of accessory REE-bearing minerals (e.g., xenotime, zircon, apatite) or subtle analytical and normalization effects. These features do not alter the overall fractionation trend and are interpreted as secondary variations superimposed on the primary sedimentary REE signature.

Although REEs are often considered relatively immobile under low-temperature sedimentary conditions, their behavior may be influenced by complexation with carbonate, sulfate, and phosphate ligands in groundwater systems. Such processes can lead to localized middle-REE enrichment or redox-driven cerium anomalies, particularly in roll-front environments. These effects are not dominant in the studied samples but are acknowledged as part of a more comprehensive REE geochemical framework.

In contrast to magmatic systems, where plagioclase crystallization plays a key role in controlling europium fractionation, sedimentary uranium systems lack such crystallization

processes, leading to smoothing of REE anomalies. As a result, the REE distribution curves exhibit weakly expressed or near-neutral europium anomalies. There are no physicochemical conditions favorable for selective mobilization or fixation of europium, in contrast to magmatic systems where plagioclase crystallization removes Eu^{2+} into the solid phase. Unlike magmatic fluids, sedimentary and groundwater systems do not promote selective redox-controlled mobilization or precipitation of europium, including Eu^{2+} species, which further contributes to the absence of pronounced Eu anomalies. REEs are transported predominantly as cations and are sorbed onto mineral or colloidal phases (e.g., clay minerals) without a strong fractionating mechanism.

Figure 2 presents chondrite-normalized REE distribution patterns for uranium ore reference materials supplied by Ore Research & Exploration, representing uranium deposits from Tanzania and Australia.

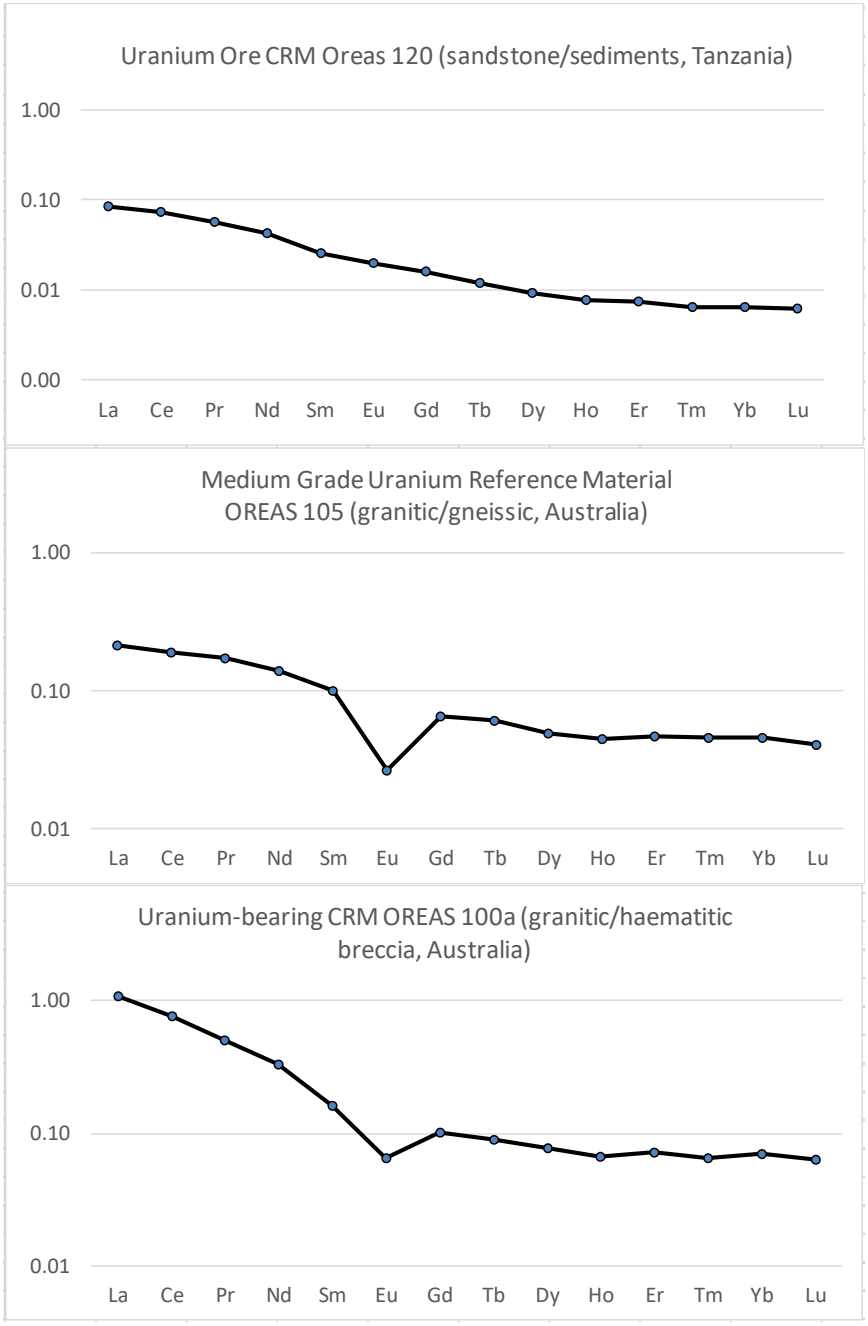


Figure 2. Chondrite C1-normalized REE distribution patterns of uranium ore reference materials (OREAS 120, OREAS 100a, and OREAS 105) from Tanzania and Australia.

The OREAS 120 uranium ore reference material exhibits pronounced fractionation of light REEs, with $(La/Yb)_n \approx 13$ and $(Gd/Yb)_n \approx 2.4$. The OREAS 100a standard is also characterized by strong enrichment in light lanthanides. In contrast, the OREAS 105 standard displays a more uniform REE distribution, closely resembling the profiles observed in core samples from uranium deposits in Kazakhstan. This similarity confirms their geochemical affinity and reflects comparable conditions of crystallization, subsequent recrystallization, and superimposed processes.

Rare earth elements are generally considered to be relatively immobile and tend to inherit the distribution characteristics of their parent rocks. Geochemically coherent REE patterns are therefore particularly valuable as petrogenetic indicators, as their ionic radii vary systematically across the series, while europium anomalies in minerals may provide insights into the redox conditions prevailing during crystallization. The relatively slow diffusion rates of rare earth and rare elements, their contrasting partitioning among metamorphic minerals, and their sensitivity to physicochemical conditions make REEs robust tracers of geological processes.

Figure 3 presents a histogram of the principal REE fractionation parameters for core materials from uranium deposits in Kazakhstan and Ore Research & Exploration reference materials, normalized to chondrite values.

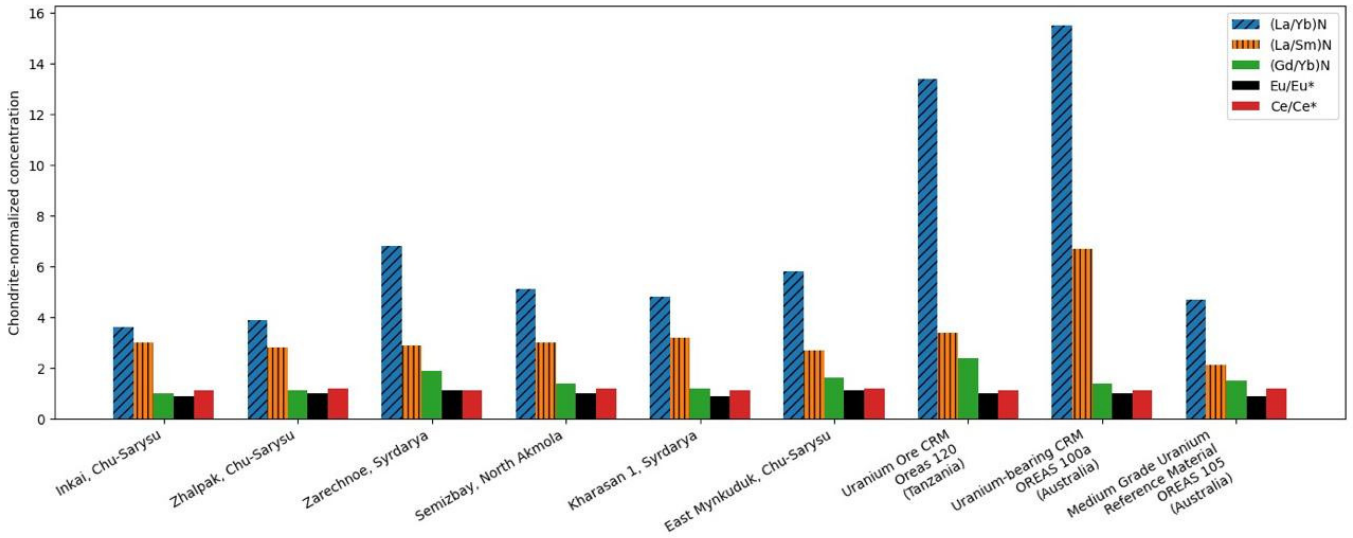


Figure 3. REE fractionation parameters (La/Yb, Gd/Yb, and Eu/Eu) in core materials from uranium deposits in Kazakhstan and Ore Research & Exploration ore reference materials, normalized to chondrite C1 [27].

Negative europium anomalies commonly reflect redox-controlled fractionation and mineralogical inheritance from source rocks [32,33]. For uranium ores, the Ce anomaly is more diagnostic in most cases, but the Eu anomaly becomes key when determining the contribution of a magmatic source or high-temperature stage. Uranium migrates as U^{6+} under oxidizing conditions and precipitates during reduction (U^{4+}). Cerium is the only rare earth metal capable of existing in two stable valence states. Therefore, the Ce/Ce (normalized) ratio is a direct indicator of the redox regime that controls uranium mineralization. In magmatic systems, europium may occur as Eu^{2+} under reducing conditions and is preferentially incorporated into plagioclase due to charge and ionic radius similarity with Ca^{2+}. Removal of plagioclase during crystallization results in depletion of europium in the residual melt and the development of a negative Eu anomaly [32]. In sedimentary systems, weak or subdued europium anomalies are typically inherited from felsic source rocks and may be further attenuated during low-temperature groundwater transport [32,33].

As the crystallization temperature of uraninite decreases below approximately 350 °C, the influence of crystal-chemical constraints increases, favoring incorporation of REEs with ionic radii close to that of U^{4+} (e.g., Tb–Er). This results in relative enrichment of the ore in middle REEs [32]. Magmatic uranium ores display a pronounced negative europium anomaly, which may be associated with inheritance of the geochemical characteristics of the parental magma. During magma crystallization, europium in the form of Eu^{2+} was preferentially incorporated into plagioclase, thereby depleting the residual melt in Eu. In natural systems, including magmatic rocks, europium occurs in both divalent and trivalent states. Compared with Eu^{3+} and neighboring trivalent lanthanides, Eu^{2+} has a larger ionic radius [33]. Subsequently, uranium mineralization formed from magmatic and hydrothermal fluids inherited this REE distribution pattern, resulting in a negative europium anomaly within the ore zone.

To compare REE fractionation characteristics in sandstone- and magmatic uranium ores, a linear regression analysis was performed following the methodology described in Ref. [9]. Linear regression analysis of REE/ΣREE is one of the most informative and cost-effective statistical tools for studying uranium ores of various genetic types. The advantage of this method is that it reflects fundamental geochemical patterns, is robust to concentration variations, allows for the classification of uranium ores by genesis, and is sufficiently informative for primary genetic interpretation. Linear regression analysis of REE/ΣREE allows for the diagnosis of redox conditions, the separation of magmatic contribution from infiltration, and the assessment of the degree of hydrothermal redistribution. The analysis is based on normalized ratios of individual REE contents to the total REE content, with prior normalization to chondritic values. This approach eliminates the influence of absolute concentration differences and focuses exclusively on the distribution patterns and fractionation behavior of REEs in the studied rocks.

The linear regression analysis of chondrite-normalized REE ratios is applied here as a comparative tool that emphasize relative element distributions rather than absolute concentrations. By normalizing individual REE abundances to the total REE content (ΣREE), the approach highlights fractionation patterns while minimizing the influence of bulk compositional differences between samples.

It is acknowledged that ratio-based datasets may be affected by closure effects and mathematical artifacts. Accordingly, the observed linear relationships are not interpreted as direct expressions of specific physicochemical processes, but rather as indicators of similarity or divergence in REE distribution patterns between uranium deposits of different genetic types.

The regression model ensures comparability between deposits with different geochemical backgrounds, as each object contributes equally to the overall characterization. Relative concentrations (e.g., La/ΣREE, Gd/ΣREE, Eu/ΣREE, etc.) therefore become dominant parameters, making the method particularly informative for comparing rocks of different origins (sedimentary versus magmatic) and different host matrices.

Figures 4–6 present the results of regression-based comparisons of REE distribution patterns in Ore Research & Exploration reference materials (OREAS 120, OREAS 100a, and OREAS 105) with core samples from uranium deposits in Kazakhstan. This approach allows visualization of similarities in REE signatures and identification of genetic affinities or distinctions between the studied samples and reference materials of well-established origin.

The REE distribution signatures of the three Ore Research & Exploration reference materials (OREAS 120, OREAS 100a, and OREAS 105), despite their well-established provenance, were treated as “unknowns” within the framework of method validation. The results demonstrate a high degree of correlation with cores from sandstone-hosted uranium

deposits in Kazakhstan, particularly for the OREAS 120 and OREAS 100a standards, thereby confirming the effectiveness of the proposed approach.

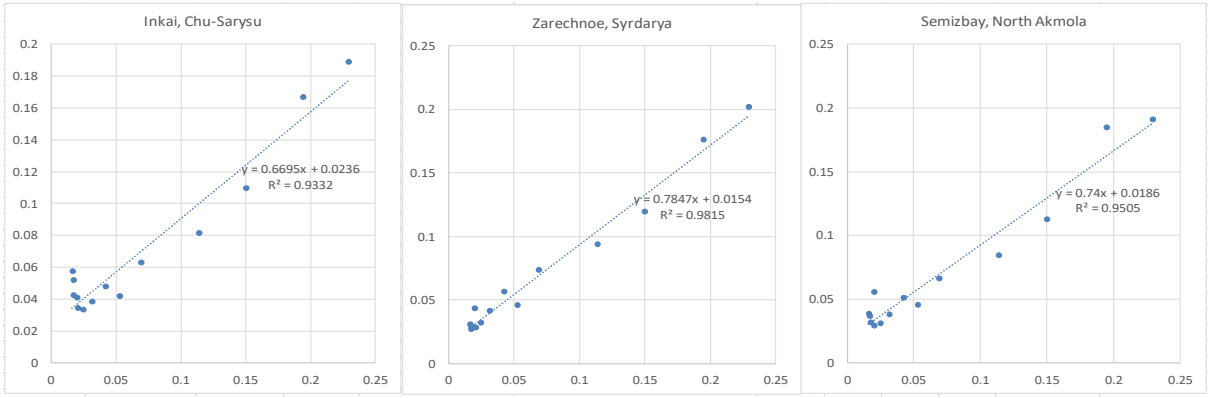


Figure 4. Regression-based comparison of normalized REE distribution patterns between the sandstone-hosted uranium ore reference material OREAS 120 and core samples from uranium deposits in Kazakhstan.

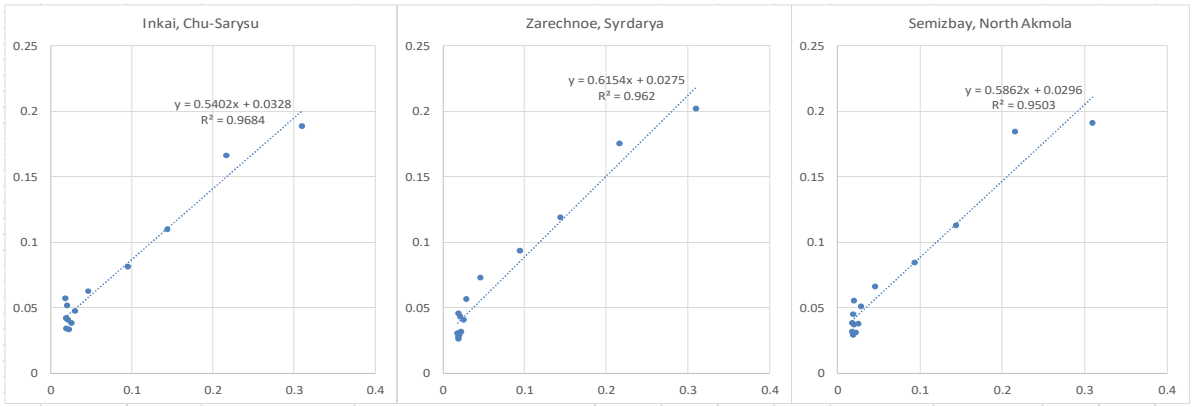


Figure 5. Regression-based comparison of normalized REE distribution patterns between the granite-hosted uranium ore reference material OREAS 100a and uranium deposits in Kazakhstan.

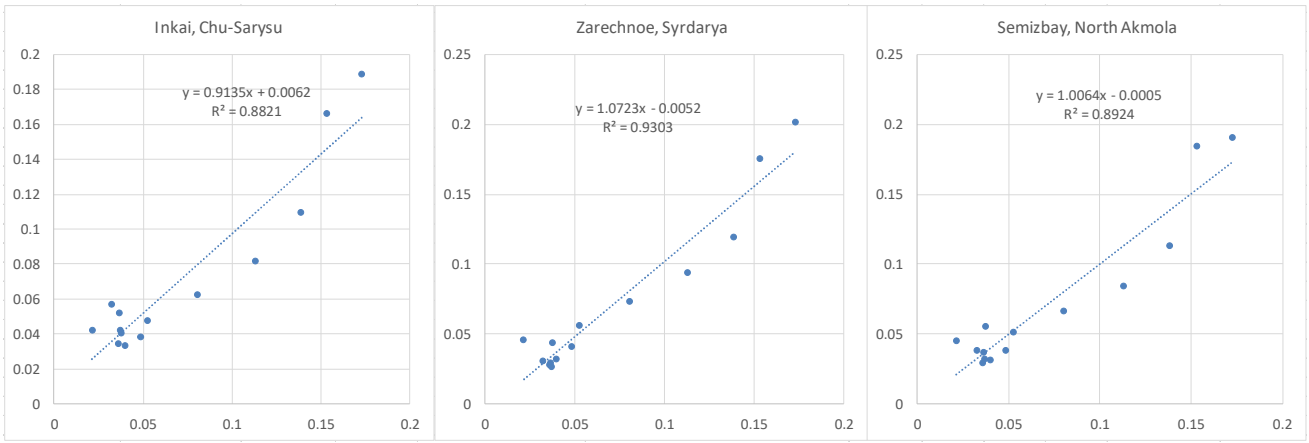


Figure 6. Regression-based comparison of normalized REE distribution patterns between the granite-hosted uranium ore reference material OREAS 105 and core samples from uranium deposits in Kazakhstan.

Owing to the high sensitivity of REEs to geochemical conditions, even at low concentrations, they exhibit well-defined zonal distribution profiles in metamorphic and sedimentary

minerals. This makes REEs powerful indicators of rock evolution, especially in cases where major elements fail to provide unambiguous interpretations [18,34].

4. Conclusions

The geochemical interpretations presented here are consistent with established REE behavior in sedimentary rocks. Their value lies in the applied comparison of deposit types using a unified analytical and statistical framework.

The developed rapid method for microwave digestion of sandstone-hosted uranium ores followed by REE determination has demonstrated high efficiency and suitability for routine analytical applications. The method provides rapid digestion, low reagent consumption, and high recovery yields, making it preferable to conventional acid digestion techniques.

Validation of the method using certified reference materials from Ore Research & Exploration (OREAS 120, OREAS 100a, and OREAS 105) showed good agreement between measured and certified values within confidence intervals. This confirms both the accuracy of the measurements and the completeness of sample digestion.

Investigation of core samples from six uranium deposits in Kazakhstan revealed characteristic REE distribution features typical of sandstone-hosted uranium ores, including enrichment in light rare earth elements, weak differentiation between middle and heavy REEs, and a subdued negative europium anomaly ($Eu/Eu^* \approx 0.7$), reflecting sedimentary genesis and remobilization under redox-gradient conditions.

For comparative purposes, linear regression analysis of normalized REE distributions was performed for ore reference materials and core samples. The results indicate that ores (OREAS 100a) exhibit a clear correlation between uranium content and heavy REEs (Tb–Er), associated with their co-incorporation into accessory minerals of granitic rocks, whereas sandstone-hosted ores (OREAS 120 and Kazakhstan deposits) display more uniform REE distributions and weak correlations with uranium content, reflecting the dominant role of groundwater-related processes and adsorption onto clay minerals.

Thus, REE distribution patterns can serve as robust geochemical indicators of uranium mineralization type.

Sandstone-hosted uranium deposits are characterized by the migration of uranium and rare earth elements in oxidizing groundwater systems, followed by precipitation upon transition to reducing environments. In sandstone deposits, the composition of REE is determined mainly by detrital minerals, for example, accessory minerals formed as a result of weathering and mechanical transfer of monazite, zircon, and xenoid from bedrock during sedimentation and basin formation.

In magmatic uranium deposits, many accessory minerals may crystallize at late stages due to the accumulation of incompatible elements, although some accessory phases may also form at earlier stages of magmatic evolution. These deposits typically feature the inclusion of rare earth elements in stable accessory phases such as monazite, allanite, and apatite, a pronounced negative europium anomaly inherited from plagioclase fractionation in granitic melts, and, under oxidizing conditions, the potential for the development of positive cerium anomalies.

Fractionation is clearly caused by geochemical processes that have occurred over millions of years under the influence of redox processes. Fractionation intensifies during the transition from sedimentary to hydrothermal rock types. Eu and Ce anomalies are key indicators of redox conditions. The primary controls on REE distribution in sandstone ores are sorption and the redox barrier.

Author Contributions: Conceptualization, Z.K., B.T. and K.T.; methodology, Z.K., B.T. and K.T.; software, K.Z., B.M., M.K. and K.S.; validation, Z.K., B.T. and K.T.; formal analysis, K.Z. and B.M.; investigation, Z.K., B.T. and K.T.; resources, K.Z., B.M. and K.S.; data curation, Z.K. and B.T.; writing—original draft preparation, Z.K., B.T., K.T. and K.Z.; writing—review and editing, Z.K., K.T., B.M. and K.S.; visualization, B.T.; supervision, Z.K.; project administration, Z.K.; funding acquisition, Z.K. All authors have read and agreed to the published version of the manuscript.

Funding: This research was funded by the Science Committee of the Ministry of Science and Higher Education of the Republic of Kazakhstan (Grant No. AP22785533—Development of an effective technology for extracting scandium from process solutions of well production).

Data Availability Statement: The data are contained within the article.

Conflicts of Interest: The authors declare no conflicts of interest. Zhiger Kenzhetaev, Bolatbek Toksanbayev and Kudaibergen Zhapabayev are employees of Ascore, 30/10 Konaev Str., Tausamaly microdistrict, Almaty, Kazakhstan. The paper reflects the views of the scientists and not the company. The funders had no role in the design of the study; in the collection, analyses, or interpretation of data; in the writing of the manuscript; or in the decision to publish the results.

References

1. Togizov, K.; Issayeva, L.; Muratkhanov, D.; Kurmangazhina, M.; Swęd, M.; Duczmal-Czernikiewicz, A. Rare earth elements in the Shok-Karagay ore fields (Syrymbet ore district, Northern Kazakhstan) and visualisation of the deposits using the Geography Information System. *Minerals* **2023**, *13*, 1458. [CrossRef]
2. Baratov, R.T.; Seitmuratova, E.Y.; Murtazin, E.Z.; Dautbekov, D.O.; Kelyukhov, V.N.; Shadiyev, N.S.; Mashrapova, M.A. Lithium Concentrations in Saline Brines of the Shu–Sarysu Depression. *Appl. Sci.* **2024**, *14*, 5351. [CrossRef]
3. Cuney, M. The extreme diversity of uranium deposits. *Miner. Depos.* **2008**, *44*, 3–9. [CrossRef]
4. Debruyne, D.; Hulsbosch, N.; Muchez, P. Unraveling rare earth element signatures in hydrothermal carbonate minerals using a source-sink system. *Ore Geol. Rev.* **2016**, *72*, 232–252. [CrossRef]
5. Qbau, N.; Nam, N.D.; Ca, N.X.; Hien, N.T. The crack healing effect of scandium in aluminum alloys during laser additive manufacturing. *J. Manuf. Process.* **2020**, *50*, 241–246. [CrossRef]
6. Petukhov, O.F.; Ruziev, B.T.; Sharafutdinov, U.Z. Recovery of rare earths from uranium leach solutions. *Min. Inf. Anal. Bull.* **2021**, *1*, 58–67. [CrossRef]
7. Doriomedov, M.S.; Sevastyanov, D.V.; Shein, E.A. Technological, institutional and economic trends in the industry of rare and rare-earth metals (review). *Proc. VIAM* **2019**, *7*, 3–11. [CrossRef]
8. Khawassek, Y.M.; Eliwa, A.A.; Haggag, E.S.A.; Omar, S.A.; AbdelWahab, S.M. Adsorption of rare earth elements by strong acid cation exchange resin thermodynamics, characteristics and kinetics. *SN Appl. Sci.* **2019**, *1*, 51. [CrossRef]
9. Spano, T.L.; Simonetti, A.; Wheeler, T.; Carpenter, G.; Freet, D.; Balboni, E.; Dorais, C.; Burns, P.C. A novel nuclear forensic tool involving deposit type normalized rare earth element signatures. *Terra Nova* **2017**, *29*, 294–305. [CrossRef]
10. Orteca, G.; Sinnes, J.P.; Rubagotti, S.; Iori, M.; Capponi, P.C.; Piel, M.; Rösch, F.; Ferrari, E.; Asti, M. Gallium-68 and scandium-44 labelled radiotracers based on curcumin structure linked to bifunctional chelators: Synthesis and characterization of potential PET radiotracers. *J. Inorg. Biochem.* **2020**, *204*, 110954. [CrossRef]
11. Rakishev, B.; Kenzhetaev, Z.; Mataev, M.; Togizov, K. Improving the efficiency of downhole uranium production using oxygen as an oxidizer. *Minerals* **2022**, *12*, 1005. [CrossRef]
12. Faizullina, S.; Isaeva, A.; Matkarimova, L.; Zhuzbaeva, A. Aspects of sustainable development of industry in Kazakhstan. In Proceedings of the E3S Web of Conferences, Milan, Italy, 13–15 February 2019. [CrossRef]
13. Khomenko, O.; Rudakov, D.; Lkhagva, T.; Sala, D.; Buketov, V.; Dychkovskyi, R. Managing the horizon-oriented in-situ leaching for the uranium deposits of Mongolia. *Rud.-Geol.-Naft. Zb.* **2023**, *38*, 49–60. [CrossRef]
14. Togizov, K.; Kenzhetaev, Z.; Muzapparova, A.; Bainiyazov, S.; Raushanbek, D.; Yaremkiv, Y. Selection of optimal parameters for chemical well treatment during in situ leaching of uranium ores. *Minerals* **2025**, *15*, 811. [CrossRef]
15. Taylor, S.R.; McLennan, S.M. *The Continental Crust: Its Composition and Evolution*; Blackwell Scientific Publications: Oxford, UK, 1985.
16. Rollinson, H. *Using Geochemical Data: Evaluation, Presentation, Interpretation*; Longman Scientific & Technical: London, UK, 1993.
17. McLennan, S.M. Rare earth elements in sedimentary rocks: Influence of provenance and sedimentary processes. *Rev. Mineral. Geochem.* **1989**, *21*, 169–200.
18. Henderson, P. *Rare Earth Element Geochemistry*; Elsevier: Amsterdam, The Netherlands, 1984.

19. Bau, M.; Dulski, P. Distribution of yttrium and rare-earth elements in the Penge and Kuruman iron-formations, Transvaal Supergroup, South Africa. *Precambrian Res.* **1996**, *79*, 37–55. [CrossRef]
20. Laverov, N.P. *Underground Leaching of Polymetallic Ores*; Academy of Mining Sciences: Moscow, Russia, 1998; 446p. Available online: https://www.geokniga.org/books/7179 (accessed on 1 July 1998).
21. Plasil, J. Oxidation–hydration weathering of uraninite: The current state-of-knowledge. *J. Geosci.* **2014**, *59*, 99–114. [CrossRef]
22. Lyashenko, V.; Dudar, T.; Stus, V.; Shapovalov, V. Justification of efficiency and subsoil protection during underground development of ore deposits using traditional technologies in combination with metals leaching. *Miner. Resour. Ukr.* **2024**, *2*, 69–77. [CrossRef]
23. Reynier, N.; Gagné-Turcotte, R.; Coudert, L.; Costis, S.; Cameron, R.; Blais, J.F. Bioleaching of uranium tailings as secondary sources for rare earth elements production. *Minerals* **2021**, *11*, 302. [CrossRef]
24. Finch, R.; Murakami, T. Systematics and Paragenesis of Uranium Minerals. In *Uranium: Mineralogy, Geochemistry and the Environment*; Burns, P.C., Finch, R.J., Eds.; Reviews in Mineralogy & Geochemistry; Mineralogical Society of America: Chantilly, VA, USA, 1999; Volume 38, pp. 91–180.
25. Toksanbayev, B.Z.; Torebekov, A.K. Method for Preparing Samples of Uranium Ores and Sandstone-Type Core Materials for Spectrometric Analysis. Patent for Utility Model No. 4046, 7 June 2019. Available online: https://gosreestr.kazpatent.kz/ (accessed on 12 January 2026).
26. Available online: https://www.oreas.com/ (accessed on 12 January 2026).
27. McDonough, W.F.; Sun, S.-S. The composition of the Earth. *Chem. Geol.* **1995**, *120*, 223–253. [CrossRef]
28. Oitseva, T.; Serikbayev, D.; Mizernaya, M.; Oitseva, T.; Mizernaya, A.M.; Kuzmina, P.O. Prospects of the Medvedko-Akhmetkinsky ore field for rare metal lithium mineralization (East Kazakhstan). In Proceedings of the 23rd International Multidisciplinary Scientific GeoConference SGEM, Albena, Bulgaria, 3–9 July 2023.
29. Amralinova, B.; Agaliyeva, B.; Lozynskyi, V.; Frolova, O.; Rysbekov, K.; Mataibaeva, I.; Mizernaya, M. Rare-Metal Mineralization in Salt Lakes and the Linkage with Composition of Granites: Evidence from Burabay Rock Mass (Eastern Kazakhstan). *Water* **2023**, *15*, 1386. [CrossRef]
30. D'yachkov, B.A.; Bissatova, A.Y.; Mizernaya, M.A.; Khromykh, S.V.; Oitseva, T.A.; Kuzmina, O.N.; Zimanovskaya, N.A.; Aitbayeva, S.S. Mineralogical Tracers of Gold and Rare-Metal Mineralization in Eastern Kazakhstan. *Minerals* **2021**, *11*, 253. [CrossRef]
31. Dyachkov, B.A.; Aitbayeva, S.S.; Mizernaya, M.A.; Amralinova, B.B.; Bissatova, A.E. New data on non-traditional types of East Kazakhstan rare metal ore. *Nauk. Visnyk Natsionalnoho Hirnychoho Universytetu* **2020**, *4*, 11–16. [CrossRef]
32. Gao, S.; Wedepohl, K.H. The negative Eu anomaly in Archean sedimentary rocks: Implications for decomposition, age and importance of their granitic sources. *Earth Planet. Sci. Lett.* **1995**, *133*, 81–94. [CrossRef]
33. Mercadier, J.; Cuney, M.; Lach, P.; Boiron, M.-C.; Bonhoure, J.; Richard, A.; Leisen, M.; Kister, P. Origin of Uranium Deposits Revealed by Their Rare Earth Element Signature. *Terra Nova* **2011**, *23*, 264–269. [CrossRef]
34. Zheltova, G.A.; Gluchshenko, V.N.; Kips, R.; Krasnopyorova, M.V.; Zheltov, D.A.; Milts, O.S.; Silachyov, I.Y.; Panova, E.N.; Toksanbayev, B.Z.; Baltabaev, A.Z.; et al. Complex of methods for analytical study of uranium-containing raw materials for nuclear forensics purpose. In Proceedings of the 2nd International Conference on Radioanalitical and Nuclear Chemistry, Budapest, Hungary, 5–10 May 2019.

Disclaimer/Publisher's Note: The statements, opinions and data contained in all publications are solely those of the individual author(s) and contributor(s) and not of MDPI and/or the editor(s). MDPI and/or the editor(s) disclaim responsibility for any injury to people or property resulting from any ideas, methods, instructions or products referred to in the content.